Small angle x-ray scattering measurements of lithographic patterns with sidewall roughness from vertical standing waves

Chengqing Wang, Ronald L. Jones, Eric K. Lin, and Wen-Li Wu[a)]
Polymers Division, National Institute of Standards and Technology, Gaithersburg, Maryland 20899

Jim Leu
Department Materials Science and Engineering, National Chiao Tung University, Hsinchu 300, Taiwan

(Received 16 March 2007; accepted 14 April 2007; published online 10 May 2007)

Small angle x-ray scattering (SAXS) measurements are used to quantify the wavelength and amplitude of the sidewall roughness in a lithographic line:space pattern due to vertical standing waves present during the photoresist exposure. Analytic equations are derived to model the x-ray scattering intensity and are used to determine the periodicity and amplitude of the standing wave roughness. The average periodicity, or pitch, and the linewidth were $L=422\pm1$ nm and $w_0=148\pm1$ nm. The period and amplitude of the standing wave roughness were $\lambda_s=65\pm1$ nm and $A_s=3.0\pm0.5$ nm. These results demonstrate the potential of SAXS measurements to quantify nondestructively and quantitatively dimensional deviations from an ideal structure. © *2007 American Institute of Physics*. [DOI: 10.1063/1.2737399]

The production of nanoscale structures, in the semiconductor industry and advanced technology applications, requires methods to measure their dimensions and quality with nanometer resolution. The semiconductor industry has identified the development of nondestructive, production-ready measurements of device structure critical dimension (CD), linewidth, height, sidewall angle, line edge roughness, and linewidth roughness as a difficult challenge for sub-32 nm technology nodes. Well-defined line edge roughness measurements are needed because excessive roughness of the structures can compromise device performance and production yield. For example, roughness induced by standing waves results in a loss of linewidth control and can lead to nonuniform etching of the underlying substrate and a loss in device functionality.[1] Currently, progress is being made with advances in optical scatterometry and scanning electron microscopy (SEM) algorithms. However, the options for characterization of the vertical sidewall roughness are generally limited including cross-sectional SEM,[2–4] a destructive technique, and atomic force microscopy,[5] a technique with limited application in dense features. Recently, critical dimension small angle x-ray scattering (CD-SAXS) was introduced as a potential method to quickly and nondestructively measure the critical dimensions (periodicity and linewidth) and the cross-sectional profile (sidewall angle and pattern height) of line gratings.[6,7]

In this letter, we demonstrate that CD-SAXS measurement can be used to determine parameters describing vertical standing wave effects in lithographic structures; a model for line edge or sidewall roughness. CD-SAXS data are obtained from lithographic lines containing a periodic roughness along the sidewalls that results from the development of a photoresist exposed to standing waves oriented perpendicular to a reflective substrate. Without an effective antireflective coating, the interference of the incoming and reflected radiations creates a standing wave of light intensity in the photoresist. The variation in intensity as a function of depth creates a periodic roughness with a mirror symmetry, as depicted in Fig. 1.[8] A test pattern was fabricated from an imaged photoresist on a 300 mm diameter wafer using a 193 nm wavelength exposure tool. Immersion in an aqueous base developer, followed by subsequent rinsing with water, produced a dense array of ≈200 nm lines separated by ≈200 nm spaces. SEM images of the line cross section (Fig. 2) reveal line edges with a periodic sidewall roughness indicative of standing waves. The lack of periodic roughness in some line edges is likely due to smearing during the cross-section sample preparation process, the heterogeneity of the developing process, or the heterogeneity in the chemistry of the photoresist.

SAXS data from the line grating test pattern were collected at the 5-ID-DND beamline at the Advanced Photon Source, part of Argonne National Laboratory. The data were collected in transmission through the silicon substrate using x-rays with an energy of 17 keV. Scattering from the line grating can be measured because the sample is well within the diffraction limit with the subnanometer x-ray wavelength λ_x is 0.0729 ± 0.0003 nm.[9] Scattered x rays were collected on a two-dimensional charge coupled device detector with a sample-to-detector distance of 719.3 ± 0.5 cm. Samples were measured as a function of the sample rotation angle ω over a range of $-30°$ to $+30°$ in $1°$ increments, where $\omega=0°$ is defined by normal incidence of the beam to the substrate. Box averages of the two-dimensional data along the diffraction axis provided $I(q)$ for each angle to create a matrix function $I(q,\omega)$, where $q=4\pi/\lambda_x \sin(\theta)$ and 2θ is the scat-

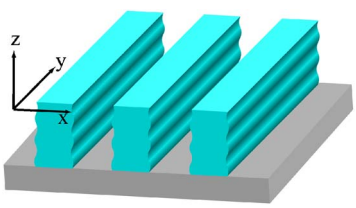

FIG. 1. (Color online) Illustration of the resulting sinusoidal roughness pattern after development of photoresists where a standing wave of light intensity exists during imaging. For the model developed here, the line is assumed to be homogeneous along y with a sinusoidally varying linewidth along z.

[a)]Author to whom correspondence should be addressed; electronic mail: wenli@nist.gov and wwu@nist.gov

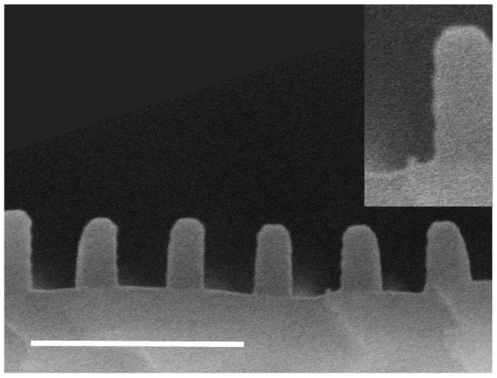

FIG. 2. Cross-sectional SEM image of the photoresist line grating used in this study. The bar indicates a length of 1 μm. The left edge of the line second from the right is blown up in the inset, showing the periodic component of the roughness.

tering angle. The data were then converted to $I(q_x,q_z)$ using a standard rotation matrix. Further details about the SAXS procedure and data analysis are provided elsewhere.[7]

The standing wave along the profile's vertical axis is well approximated by a simple sinusoidal wave form.[10] The sidewall of a patterned line grating is modeled as a sinusinodal wave form, where the z axis is normal to the substrate and has an origin at the substrate plane, the x axis is normal to the average sidewall, and the y axis is parallel to the lines. Variations in linewidth occur only along the z axis and the lines are assumed to be homogeneous parallel to the y axis. The depth dependent width of the line is $w(z)=w_r(z)-w_l(z)$, where $w_r=w_0/2+A_s\sin(2\pi z/\lambda_s+\phi_s)$ and $w_l=-w_0/2-A_s\sin(2\pi z/\lambda_s+\phi_s)$, where A_s, λ_s, and ϕ_s are the amplitude, wavelength, and phase of the standing wave roughness, respectively, and w_0 is the average linewidth. For simplicity, we set $\phi_s=0$. The corresponding cross-sectional profile in Fourier space, the form factor $f(q_x,q_z)$, is given by Eq. (1)

$$f(q_x,q_z)=i\frac{e^{-iq_xw_0/2}}{q_x}\int_0^h e^{-i(q_zz+q_xw_s)}dz - i\frac{e^{iq_xw_0/2}}{q_x}\int_0^h e^{-i(q_zz-q_xw_s)}dz, \tag{1}$$

where $w_s=A_s\sin(2\pi z/\lambda_s)$ and h is the height of the line gratings. Equation (1) can be simplified by introducing a variable $t=2\pi z/\lambda_s$, and setting the height of the line to be an integer product of the wavelength, that is, $h=N\lambda_s$. These expressions lead to $f(q_x,q_z)=f_1f_2$, where $f_1=\Sigma_{n=0}^{N-1}e^{iq_zn\lambda_s}$ and

$$f_2=\frac{i\lambda_{SW}}{2\pi q_x}\left(e^{-iq_xw_0/2}\int_0^{2\pi}e^{i(\nu t-\beta\sin t)}dt - e^{iq_xw_0/2}\int_0^{2\pi}e^{-i(-\nu t-\beta\sin t)}dt\right), \tag{2}$$

where $\nu=q_z\lambda_s/2\pi$ and $\beta=q_xA_s$. The integral $\int_0^{2\pi}e^{i(\nu t-\beta\sin t)}dt$ can be expressed as a combination of Anger's function $J_\nu(\beta)$ and Weber's function $E_\nu(\beta)$ of the argument β and order ν as[11]

$$\frac{1}{2\pi}\int_0^{2\pi}e^{\pm i(\nu t-\beta\sin t)}dt = \cos^2\nu\pi J_\nu(\beta)+\sin\nu\pi\cos\nu\pi E_\nu(\beta) \pm i(\sin^2\nu\pi E_\nu(\beta)+\sin\nu\pi\cos\nu\pi J_\nu(\beta)), \tag{3}$$

$J_\nu(\beta)$ and $E_\nu(\beta)$ in turn can be expressed as a series of Gamma functions.[12]

For gratings with N lines of pitch, L, and infinite length, the scattering intensity in the q_x-q_z plane is

$$I=\delta\left(q_x=\frac{2n\pi}{L}\right)\frac{\sin^2 Nq_z\lambda_s/2}{\sin^2 q_z\lambda_s/2}|f_2|^2. \tag{4}$$

The scattering intensity at $q_z=0$ is simply

$$I_0=\delta\left(q_x=\frac{2n\pi}{L}\right)\frac{\sin^2 q_xw_0/2}{q_x^2}J_0^2(\beta). \tag{5}$$

For a rectangular cross section, in the absence of sidewall roughness, the intensity along $q_z=0$ scales as $I_0^{\text{ideal}}\sim\sin^2(q_xw_0/2)/q_x^2$. In the limit of small $\beta(=q_xA_s)$, the ratio of the scattering intensity from the cross section of an ideal smooth rectangular line with periodic roughness can be expressed as a series, namely,

$$\frac{I_0}{I_0^{\text{ideal}}}\sim J_0^2(\beta)\sim 1-\frac{\beta^2}{2}+o(\beta^2)\sim 1-\frac{A_s^2}{2}q_x^2+o(A_s^2q_x^2). \tag{6}$$

The second term can be interpreted as an apparent Debye-Waller factor.[13] That is to say, the amplitude (A_s) of the standing wave roughness can be determined from the net decrease in the scattering intensity from that which would result from a smooth rectangle line profile. This amplitude A_s is a direct measure of the line edge roughness defined as

$$\langle\sigma^2\rangle=\frac{\int_0^\lambda\left(A_s\sin\frac{2\pi}{\lambda_s}z\right)^2dz}{\int_0^\lambda dz}=\frac{A_s^2}{2}. \tag{7}$$

The SAXS data from the test line grating, presented in the q_x-q_z plane in Fig. 3(a), closely resemble the calculated $I(q_x-q_z)$ in Fig. 3(b) from Eq. (4). The typical form factor of a line grating is observed from the high scattering intensity emanating from the origin. The most striking feature of the data is the two rows of high intensity bands parallel to the q_x axis at $q_z=0.95\pm0.01$ nm^{-1}. This corresponds to a standing wave roughness of periodicity $\lambda_s=65\pm1$ nm. This value is qualitatively consistent with what can be estimated from the SEM micrograph (Fig. 2). The series of small intensity maxima parallel to q_z at every scattering maxima along $q_z=0$ is observed because the pattern height, h or N, is finite, as indicated by Eq. (4). From the data along $q_z=0$, the average periodicity, or pitch, and the linewidth are determined to be $L=422\pm1$ nm and $w_0=148\pm1$ nm, respectively.[9] The fit of the data along $q_z=0$, combined with a fit of the satellite intensity bands using Eq. (6), provides the amplitude of the sidewall roughness caused by standing wave, $A_s=3.0\pm0.5$ nm.

The amplitude of the roughness can also be evaluated from Eq. (4) and the data along a fixed q_x. In Fig. 4, the scattering intensity versus q_z at $q_x=0.213$ nm^{-1} is fitted by the ideal rectangular cross-section model without any periodic roughness. In general, the features of the graph that

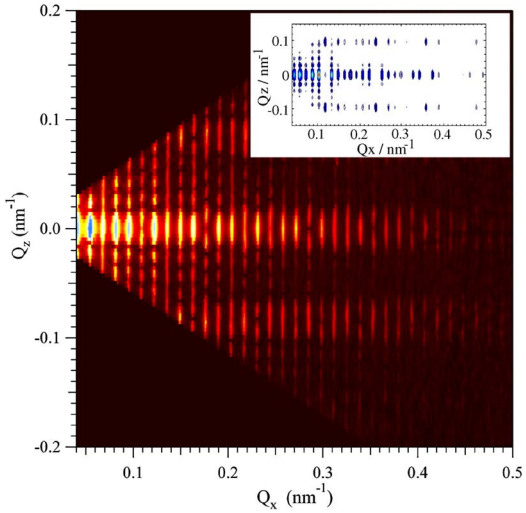

FIG. 3. (Color online) (a) Small angle x-ray scattering intensity in the q_x-q_z plane measured experimentally and calculated based on Eq. (4) (inset). The two rows of high intensity bands parallel to q_x axis at $q_z \approx 0.95 \pm 0.01$ nm^{-1} correspond to a standing wave roughness with a wavelength of $\lambda_s = 65 \pm 1$ nm. (b) Simulated scattering pattern based on the Eq. (4).

originate from the average dimensions of the line grating are well fitted by the rectangular model. However, the model does not capture the maxima at $q_z = 0.95 \pm 0.01$ nm^{-1}. This fit yields a line height of $h = 324 \pm 10$ nm. When the standing wave roughness on both sidewalls of every line is included, the fit (triangle line) between the model [Eq. (4)] and the data is reasonable. We note that the cross section of the rectangular model is different from the actual line cross section seen in Fig. 2; the actual lines appear to have rounded tops rather than sharp rectangular corners. The minor discrepancy in the fit using Eq. (4) can result from the simplification of choosing a rectangular cross-section model. The ratio of intensity of satellite peaks at $q_z = 0.95 \pm 0.01$ nm^{-1} to that at $q_z = 0$ is dictated by the amplitude of the standing wave roughness. In this case, the fit results in $A_s \approx 3$ nm, a value consistent with that estimated by the apparent Debye-Waller approach [Eq. (6)].

Finally, the characterization method outlined here can also be used to estimate the refractive index of the photoresist. The standing wave profile arises because a 180° phase

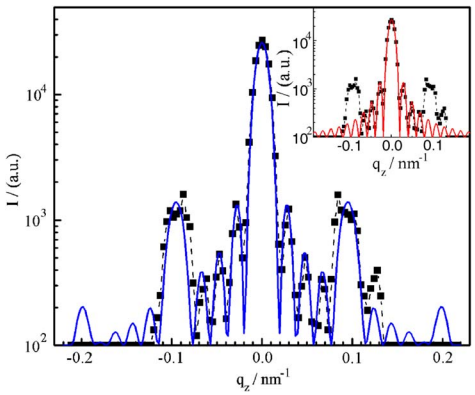

FIG. 4. (Color online) Experimental scattering intensity as a function of q_z at $q_x = 0.213$ nm^{-1} (—□—) compared to two model calculations. Shown are model data from the best fit line without periodic roughness (—○—) and the same model incorporating $A_s = 3$ nm and $\lambda_s = 65$ nm (—△—).

difference between the incident exposure beam and the reflected beam because the substrate has a higher refractive index than the photoresist. If the incident beam is normal to the substrate, the destructive interference occurs at $h = (2n - 1)\lambda_P/4$, and the constructive interference occurs at $h = (2n - 1)\lambda_P/2$. As a result, the wavelength of the standing wave in the line gratings is $\lambda_P/2$, where λ_P is the wavelength of incident beam in the photoresist with $\lambda_P = \lambda_0/n$. Based on this relationship, we estimate the refractive index of the photoresist at the exposure wavelength of 193 nm as $n = 1.47$. In this work, $N = 5$ is chosen for the calculation, where N is the number of roughness periods along the sidewall. Realistically, the number of standing waves is not an integer value. The calculations needed to include noninteger N require additional work, but does not add more physical insight to the SAXS technique and is not included here.

In summary, we demonstrate the use of SAXS to measure quantitatively the periodic sidewall roughness that results from standing waves propagating normal to the substrate during photoresist imaging. The capability of measuring roughness, deviations from an ideal structure, provides an important complement to previous work, detailing the methodology for characterizing the pitch, linewidth, height, and cross-sectional profile of line gratings that span in size from 5 to 500 nm in width. Unlike optical scatterometry or SEM measurements, this approach is readily applicable for patterns with smaller linewidths and pitches. Future work includes the development of models and methods to quantify line edge and linewidth roughness from production samples.

This work was funded in part by the NIST Office of Microelectronics Programs. Use of the Advanced Photon Source was supported by the U.S. Department of Energy, Office of Science, Office of Basic Energy Sciences, under Contract No. DE-AC02-06CH11357. This work is official contribution of National Institute of Standards and Technology.

[1] W. M. Moreau, *Semiconductor Lithography* (Plenum, New York, 1988), p. 380.
[2] F. Askary and N. T. Sullivan, Proc. SPIE **4344**, 815 (2001).
[3] A. V. Nikitin, A. Sicignano, D. Y. Yeremin, M. Sandy, and T. Goldburt, Proc. SPIE **5038**, 651 (2003).
[4] A. V. Nikitin, A. Sicignano, D. Y. Yeremin, M. Sandy, and E. T. Goldburt, Proc. SPIE **5038**, 1089 (2003).
[5] X. Qian, J. Villarrubia, F. Tian, and R. Dixson, Proc. SPIE **6518**, 651811 (2007).
[6] T. Hu, R. L. Jones, W.-L. Wu, E. K. Lin, Q. Lin, D. Keane, S. J. Weigand, and J. M. Quintana, J. Appl. Phys. **96**, 1983 (2004).
[7] R. L. Jones, T. Hu, E. K. Lin, W.-Li Wu, R. Kolb, D. M. Casa, P. J. Bolton, and G. G. Barclay, Appl. Phys. Lett. **83**, 4059 (2003).
[8] L. F. Thompson, C. G. Willson, and M. J. Bowden, *Introduction to Microlithography* (American Chemical Society, Washington, DC, 1994).
[9] The data in this letter, in the figures, and in the tables are presented along with the standard uncertainty (±) involved in the measurement, where the uncertainty represents one standard deviation from the mean.
[10] C. A. Mack, Appl. Opt. **25**, 1958 (1986).
[11] G. N. Watson, *A Treatise on the Theory of Bessel Functions*, 2nd ed., (Cambridge University Press, Cambridge, 1966), pp. 308–311.
[12] I. S. Gradshteyn and I. M. Ryzhik, in *Table of Integrals, Series and Products*, 5th ed., edited by Alan Jeffrey (Academic, New York, 1994), pp. 1002–1003.
[13] A. Guinier, *X-Ray Diffraction in Crystals, Imperfect Crystals, and Amorphous Bodies* (Dover, New York, 1994), p. 81.